

TRW Response to TPF Reference Mission Attachment X to Contract Mod 8

The TPF SWG, following the Final Architecture Review in 12/01, requested that all contractors provide information to allow a direct comparison between the architectures. They sent out a document of questions dated 04 February 2002. TRW submits this document in response.

Instrument Configuration

Below are the TRW answers to the questions posed in the first section of the Reference Mission Document. Included for convenience are the original questions.

As a minimum for each configuration, please provide the following critical instrument parameters:

1. Optical architecture (apodized aperture, coronagraph, other)

Infrared Coronagraph

2. Optical layout drawing

See the following figures for the optical layout of the telescope and coronagraphic imager. (The 4th mirror is a deformable flat with a 202 x 200 array of actuators to correct wave-front-error from $\approx 1 \mu\text{m}$ to $\approx 1 \text{nm}$).

13:18:32

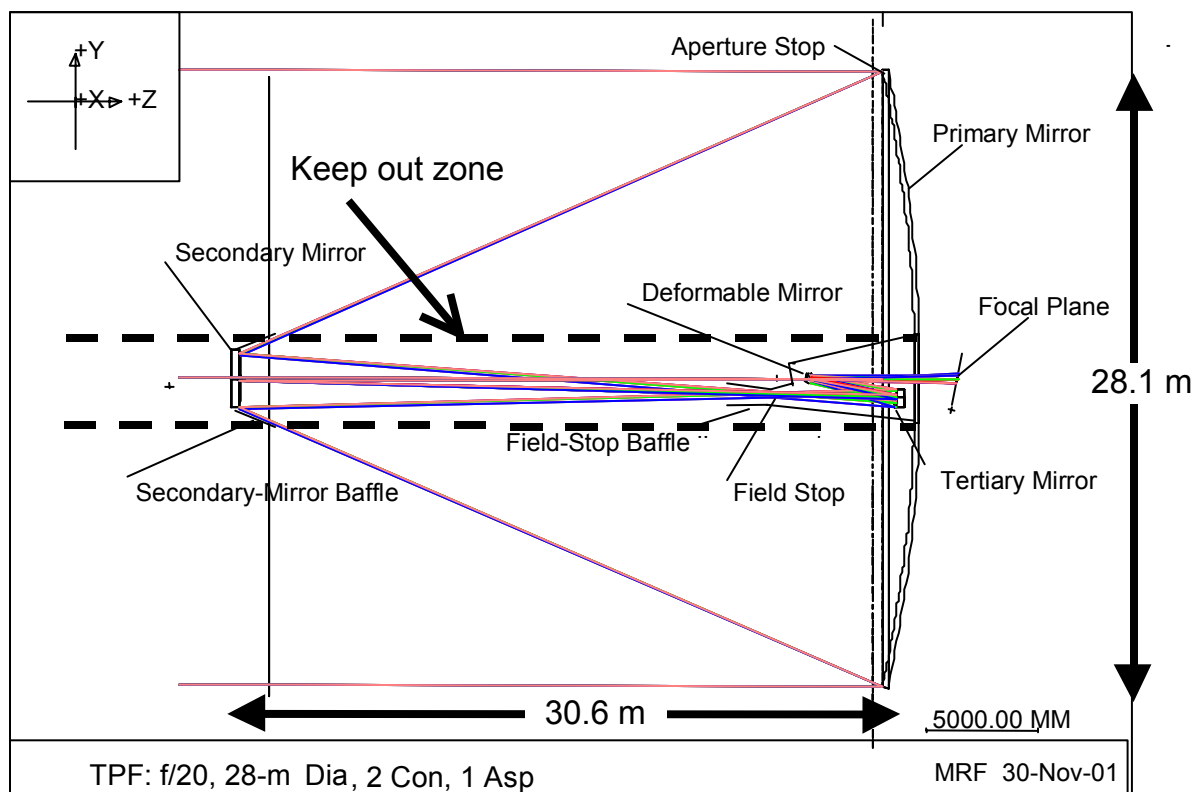


Figure 2-1: Optical layout of the Primary telescope

13:21:46

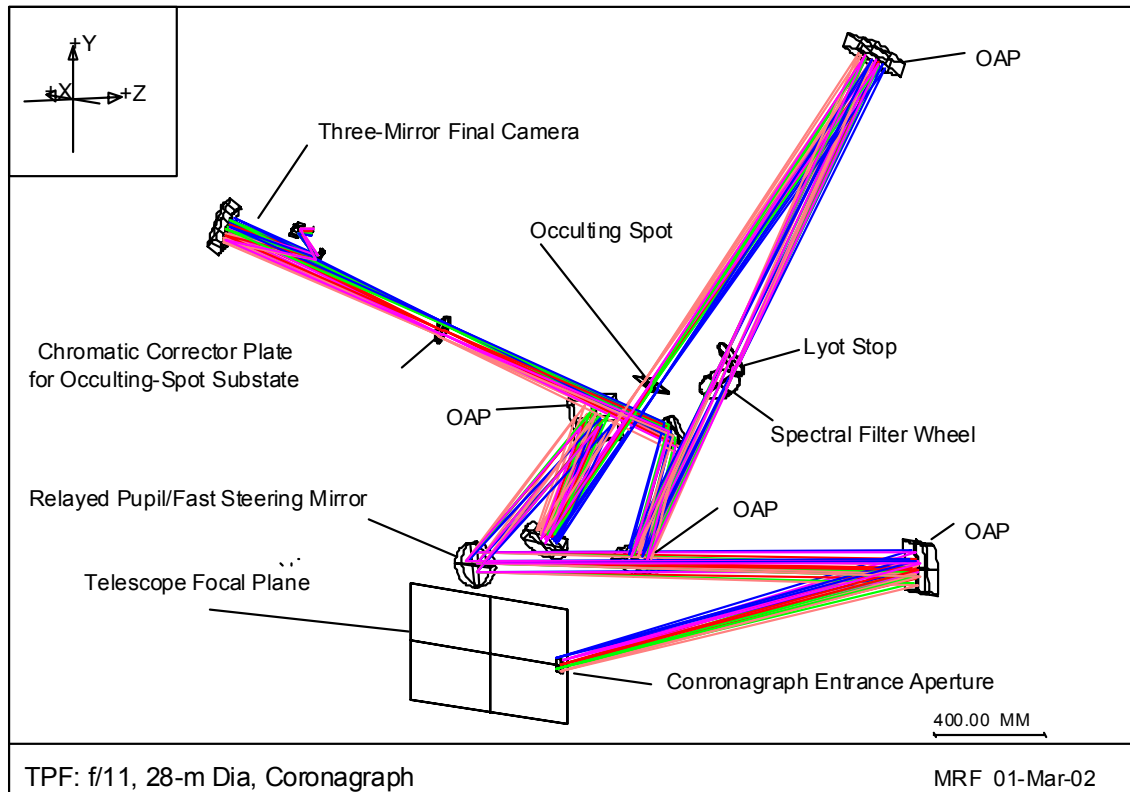


Figure 2-2: Optical layout of the coronagraphic imager instrument

3. Primary aperture shape dimensions actual area, and effective area.

28-meter, 3-mirror anastigmat, telescope with a segmented primary (36 hexagonal segments, 3.96 m flat-flat), 488.9 m² actual area. The results for the observing program were modeled using a 467 m² effective area which accounts for a simple Lyot mask that blocks the outer edges of the primary mirror and the support struts for the secondary mirror. This decision was based on modeling done by John Trauger at JPL that indicated that a simple Lyot mask would be adequate to control the diffracted star light. Detailed modeling by Bauer Associates indicates that a more aggressive Lyot mask may be necessary. For their work, an effective area of ≈ 360 m² with an apodization function on the Lyot mask was used (see below).

4. Primary aperture optical figure

See error budget (Attachment 1) and optical prescription (Attachment 2).

5. Operational wavelength range

The telescope is designed to be used across a broad wavelength range with good performance. The diffraction limit will drive the short wavelength limit of operation but 3 μ m is achievable even at the loosest tolerance of diffraction limited at 7 μ m. The long wavelength cutoff is driven by the thermal self-emission of the telescope. Since the telescope is <35K, the thermal emission does not become significant until ≈ 20 μ m and will not severely limit the sensitivity of the telescope until ≈ 30 μ m, outside the range of Si:As detectors.

The coronagraph when working in imaging (detection) mode will cover at least 7-17 μm with a goal of 3-28 μm . The coronagraph spectrometer has two modes, one covering the 6-12 μm band and the other the 12-24 μm band. The 6-12 μm band is the primary used for characterization and is used for the modeling. An optional general astrophysics imager would cover the 3-28 μm band.

6. Amplitude uniformity requirement

See error budget (Attachment 1)

7. Corrected optical figure (after AO, if an deformable mirror is used)

See error budget (Attachment 1)

8. Aperture mask shape including intensity and phase tolerances

Not applicable

9. Coronagraph mask shape including intensity and phase tolerances

The coronagraph spot shape is given by the following equation:

$$transmission(r) = \exp\left\{-8 * \ln(10) * \exp\left(\frac{-r^2}{2 * (d/2.35)^2}\right)\right\}$$

Where r is the distance from the center of the spot and d is a measure of the spot diameter. The mathematical form is an exponential of a standard Gaussian form in which d is the FWHM of the Gaussian curve. The $8 * \ln(10)$ factor sets the transmission at the center of the spot to 10^{-8} .

The physical occulting spot will be on a substrate approximately 35 mm square with the apodized spot in the center. The spot will have the transmission function of $t(r) = \exp(-18.42 * \exp(-r^2/0.0172))$ where r is the distance from the center of the substrate in millimeters. This is quite small and the errors will be critical. The physical scale the errors will be important over are on the order of $1/5^{\text{th}}$ of a pixel or 0.0136 mm at the occulting spot. We estimate that the intensity errors on this size scale need to be <1% from the perfect shape as described by the mathematical equation.

10. Lyot mask shape including intensity and phase tolerances

The Lyot mask is modeled as a simple binary form that masks the outer edges, the central obscuration, and the secondary support struts. To date, no additional masking has been required given the small gaps between the mirror segments and the properties of the occulting spot. The mask is suggested to be made of cut metal with no associated phase tolerances. The exact shape has not been shown to be critical, but alignment with the secondary support structure and central obscuration will need to be held tightly, or the mask can be oversized at the expense of throughput.

Detailed modeling by Bauer Associates suggest that a more aggressive mask may improve the Q at the planet location at the expense of overall throughput of the system. They modeled a mask that has a diameter equivalent to 26 m at the telescope primary aperture with a gaussian cutoff at the edge extending an additional 2 m in from the edge. They found that the central obscuration only needs a simple binary mask but that the outer edge is better served with this apodized shape. They also masked out an area ≈ 0.2 m at the segment edges which does not appear to be necessary. Figure 10-1 is a comparison of the stellar flux after the Lyot mask, first without an outer stop (just the central obscuration and segment junctions) and the second with the Lyot mask as described. They are shown on the same color scale.

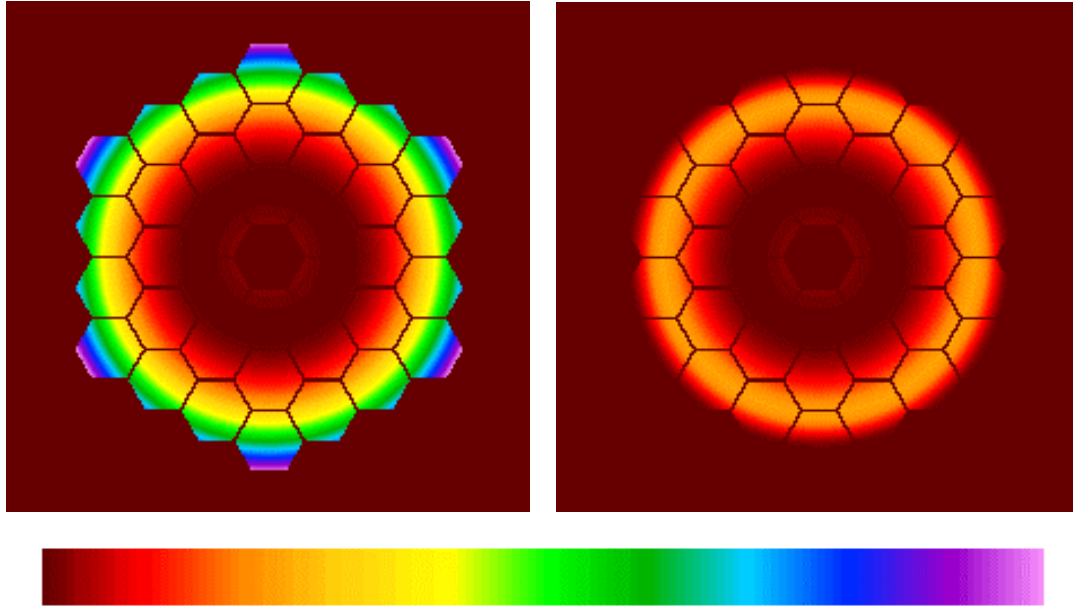


Figure 10-1: Comparison of residual star light after the Lyot mask

11. Angular resolution at planet position, in the final image (after Lyot, etc).

The sampling on the FPA is designed to be 25 mas per pixel over the entire field of view. (5 pixels for $2.44\lambda/D$ at $7\mu\text{m}$). The current field of view is 12×12 arcseconds (512 x 512-pixel detector). The telescope resolution is 89.9 milli-arcseconds at $10\mu\text{m}$. If the more aggressive Lyot mask proposed by Bauer Associates is used, the radius of the first Airy ring increases to just under 100 mas at $10\mu\text{m}$.

12. Inner and outer radius of effective field of view within which planets might be detected (instantaneous and after observations at multiple roll angles)

Based on modeling by TRW, John Trauger at JPL, and Bauer Associates, this design can detect planets at separations of >50 mas for a range of distances and stellar types. Closer than that, the planet signal is swamped by the stellar leakage. The outer radius corresponds to the extent of the focal plane array and is designed to be ≈ 6 arcseconds.

13. Operating temperatures and thermal stability for key optical components

The telescope primary mirror is ≈ 21 K average, 40 K maximum. When changing the observing attitude, the worst case hot-to-cold case ΔT of the primary mirror elements is <0.31 K, with an average of 0.23K. The secondary mirror is predicted to be 25 K and the Science Instrument Module will be 30K provided no more than 0.62 W of heat are generated in the compartment.

14. Effects of spacecraft parameters (vibration, pointing jitter, etc) on stability of PSF

See error budget (Attachment 1)

Modeling by Bauer Associates show that current requirements in the error budget have no appreciable effect on the PSF of the star as passed by the occulting spot and Lyot mask. This is shown in Figure 14-1 below.

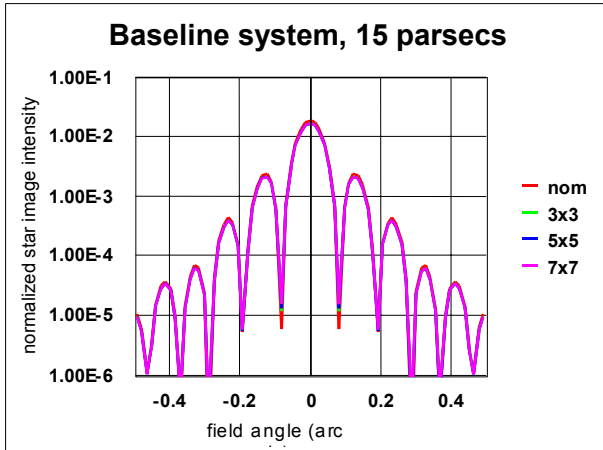


Figure 14-1: Normalized intensity (1 = maximum intensity with no masking) for 4 “smearing” cases where the “smearing” is a function that combines the effects of jitter, low frequency mirror PSD, and the zodiacal light background. Inputs for this model are 5 mas rms radius for jitter, $\lambda/10$ (@0.633 μm) primary mirror PSD, and solar system zodiacal light levels for a system at 15 pc.

15. Spectrometer design

The spectrograph portion of the coronagraph instrument is shown in Figure 15-1. It is a simple dispersive system that employs a multi-object slit mask at the image plane based on technology being developed for the NGST Multi-Object Spectrometer. Our baseline is a microshutter device, but we will incorporate the technology as validated by the NGST program. The dispersive element is tentatively identified as a grating, but it could also be a prism. The spectral resolution at the focal plane is designed to be $0.2 \mu\text{m} / \text{pixel}$ from 6 to 12 μm to cover the needed spectral band for minimal characterization. The advantage of using a grating is that it can be used in the 2nd order for the 6 – 12 μm band and in 1st order for 12 – 24 μm with a dispersion $\frac{1}{2}$ that of the shorter band ($0.4 \mu\text{m} / \text{pixel}$). Promising targets can be initially characterized in the 6 – 12 μm band, then further characterized in the 12 – 24 μm band if desired. The spectrograph will use a second 512 x 512 Si:As BIB detector, identical to the one in the imager. The required spectral coverage and available slit masks will limit the field of view of the characterization instrument. We have designed the optical system for a 8 x 8 arcsecond field of view but the slit mask may further limit the field of view to $\approx 6 \times 6$ arcseconds.

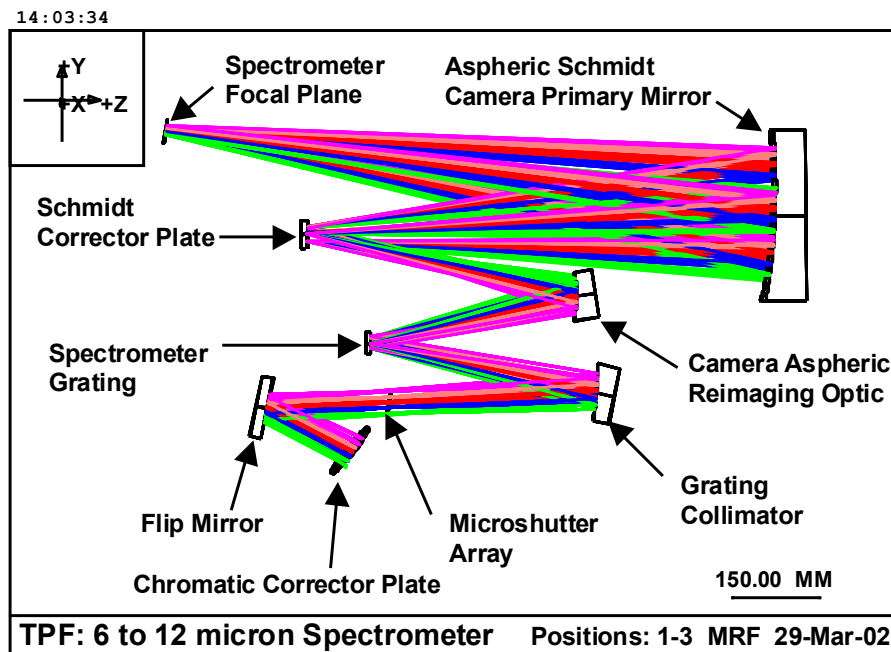


Figure 15-1: Optical layout of the coronagraph spectrometer.

16. Operations scenario

The spot and filter may change depending on the spectral type of the star and expected habitable zone, allowing a much better job to be done in a much shorter time for those target with a larger habitable zone or better contrast ratio. However, the number of spots and filters available for the detection mission is small, perhaps 4 of each.

The operation of the large aperture coronagraph for a given target is as follows:

- 1) Slew observatory to target
- 2) Acquire target with guide camera
- 3) Coarse align target to the coronagraph
- 4) Coronagraph guide system takes over (reflected starlight from occulting spot)
 - Fine Pointing Mirror corrects line of sight errors at a bandwidth of 10's of Hz.
- 5) If spectroscopic data, insert flip mirror to spectrometer optics
- 6) Select the filter to match stellar spectral type and orbit geometry (12 μm , R=5 filter is default; may switch to 10 μm , R=3 to 5, or 7 μm , R=3)
- 7) Select occulting spot
 - Log-Gaussian spot as described in question 9 with 80 mas diameter is current default
 - Larger spot diameters and/or Gaussian spots available for systems with larger habitable zones (angular size)
 - Smaller spot diameters for systems with HZ separations of <80 mas with corresponding Lyot masks optimized for the size and shape.
 - For Gaussian spots, apodized Lyot mask will also be needed
- 8) Once target is acquired, all options selected, and major dynamic modes of the observatory have been allowed to settle, start integration
 - Maximum single integration time is ≈ 1000 seconds due to cosmic ray flux (NGST result). Multiple reads expected for most observations. Data will be stored separately to allow cosmic ray removal algorithms to be applied.
 - Observatory will be rolled about the optical axis by $\approx 10^\circ$ at least once during the integration time to allow PSF subtraction. For very long observations (determined by the observing efficiency) the roll can be done multiple times. Roll may be inadvisable for some spectroscopy observations depending on the spectrometer design implemented.

Beyond this sequence, there are also calibration sequences that will update the primary mirror and deformable mirror figure using either the guide camera or a dedicated wavefront sensing camera, as well as provide photometric calibration for the instruments.

For the spectroscopy observations, the setup is the same as for imaging observations, except that a broadband 6 – 12 μm filter is used in the filter wheel and once the star image is lined up on the occulting spot, a mirror is inserted into the beam to direct the light to the spectrograph. A minimum of two apertures in the slit mask will be directed to open, one at the planet location and one on the opposite side of the star from it to permit starlight subtraction. Unless testing shows that the PSF is very asymmetrical, no roll will be used for these observations. Additional apertures in the slit mask can be opened for other objects in the field of view provided the spectra do not overlap.

17. Specify Q, defined as the operational ratio planet light/scattered starlight. What is the needed stability in the PSF/scattered light to see a planet for a given Q? Justify why you feel the instrument PSF is that stable (not necessary for configurations working at a Q of 1). The value of Q should be consistent with the properties of the optical system given above.

See figure 17-1 for mean value of Q versus radial distance from the star. The stability specified in the error budget is consistent with figure, and provides adequate performance.

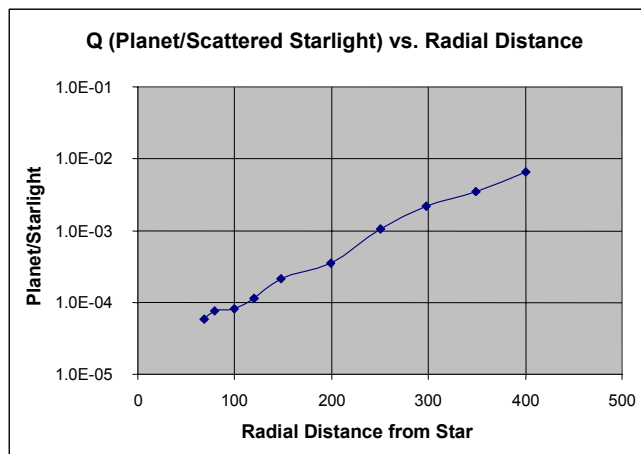


Figure 17-1: Estimated Q for the modeled Coronagraph system.

- Total optical efficiency for planetary light including reflection and transmission losses, effective vs. total collection area, Lyot mask loss, filters, etc. for both broadband and spectroscopic measurements

Broadband: The optical transmission is a function of wavelength. We have used all gold coatings on the optical elements and assumed an 80% filter transmission. This gives a total transmission is 0.67 at 12 μm . The Lyot mask losses in the TRW modeling efforts are $\approx 5\%$. This yields a total system transmission of $\approx 63\%$. This does not include the detector quantum efficiency which is approximately 0.407 at 12 μm .

Spectroscopic: The spectrometer uses the same optics as the imager, with the addition of 6 additional optical elements. The main loss in that optical train is due to the efficiency of the grating. A perfect grating has an efficiency of $\approx 80\%$. The TRW model includes additional efficiency losses in the spectrometer, yielding a total transmission of 40%. This is for a 25 mas pixel at the slit mask and cannot be applied to the total incoming flux.

- Specify detected average count rates, in the effective planetary diffraction spot size (FWHM), from planet, diffracted star, scattered star, exo-zodi, local zodi, instrument thermal emission, and detector dark counts. Assume the solar system at 10 pc.

The table below gives values for several filters that could be used during the detection mission. This has used the flux values provided by the SWG. The detector dark current is estimated to be 30 electrons per pixel so the number of the pixels in the FWHM had to be calculated. All of these values have assumed a 67% optics transmission, the 95% Lyot mask efficiency, and a detector QE of 40.7%. These values have also been multiplied by the occulting spot transmission as a function of angular distance from the stellar position. No allowances have been made for LOS pointing errors or jitter in these values.

Counts per second per FWHM of Airy disk in a 20% bandpass								
Central λ	# pixels per FWHM	planet	diffracted star	exo-zodi	endo-zodi	thermal self-emission	detector dark counts	total
7	3.8	15.4	9.302E+05	281.08	281.08	3.083E-13	112.6	9.309E+05
10	7.7	115.6	1.279E+06	1699.19	1699.19	9.628E-06	229.9	1.283E+06
11	9.3	159.7	1.286E+06	2457.44	2457.44	3.671E-04	278.1	1.292E+06
12	11.0	176.9	1.523E+06	3299.49	3299.49	7.570E-03	331.0	1.530E+06
17	22.1	149.2	5.455E+06	8394.77	8394.77	1.266E+02	664.3	5.473E+06

Observing Program

The next part of the reference mission calls for evaluating the integration time for doing key parts of the TPF mission. These are enumerated below.

1. Detection Mission

We have used the Earth spectrum provided by the SWG and summed it over a 20% wavelength band centered at 12 μm . The following table shows the required observing time for a single detection observation of the Earth in the Solar System oriented at 45 degrees to our line of sight. This is for the case of 1x the local zodiacal dust, at 12 μm , using the instrument configuration described above. The only variation is for the 15 pc case where a 60 mas occulting spot was used instead of an 80 mas one.

Case	Integration Time Required	# individual observations	Time to execute 10 degree roll	Total Observation time
3 pc	< 30 s	2	1 hour	3630 seconds
5 pc	200 s	2	1 hour	4000 s
10 pc	3325 s	4	1 hour	7000 s
15 pc	60800 s	64	3 x 1 hour = 5 hours	71600 s \approx 20 hours

No time has been allocated for initial target acquisition in these values. This will add approximately 2 hours per observation to slew, acquire, and settle. It is likely that for the large angular separation systems, using a PSF obtained from a standard star or created from observations of many sources could be used to subtract the star light. This would eliminate the need for a roll and make the short observation targets much more efficient in terms of observation time.

Using the Earth at 10 pc again, we varied the zodiacal light intensity with the results documented in the table below. The effect of the presence of zodiacal dust in the external system is minimal using this system for any expected amount of zodiacal light contribution. The ratios of increased exposure time is similar for any distance of the Earth-Sol system.

Zodi factor	Integration Time Required	# individual observations
0.5	3320 s	4
2	3330 s	4
5	3360 s	4
10	3400 s	4
25	3520 s	4
50	3760 s	4

The performance of the Large Aperture InfraRed Coronagraph (LAIRC) against the canonical systems is quite good. As the separation becomes very small, the occulting spot must be smaller. This increases the flux coming in the system and makes the dynamic range of the detector an issue. We did not include this effect in the modeling, but based on current detector technology, the integration time for the individual exposures will need to be shorter when using the smaller occulting spots. This will affect the SNR of targets outside the stellar PSF because where there is little signal, the detector will be readnoise limited. This will not affect the planet detection mission unless there are interesting planets in outer orbits.

Based on inputs from our science team and analysis of the probability of detecting a planet in a given observation given orbital dynamics and a range of inclination angles, each target should be observed 3 times during the detection mission. The timing of these observations should be phased to sample different phases of an orbital period of a potential terrestrial planet. This will have to be coordinated with the accessible part of the sky of the telescope at any given time.

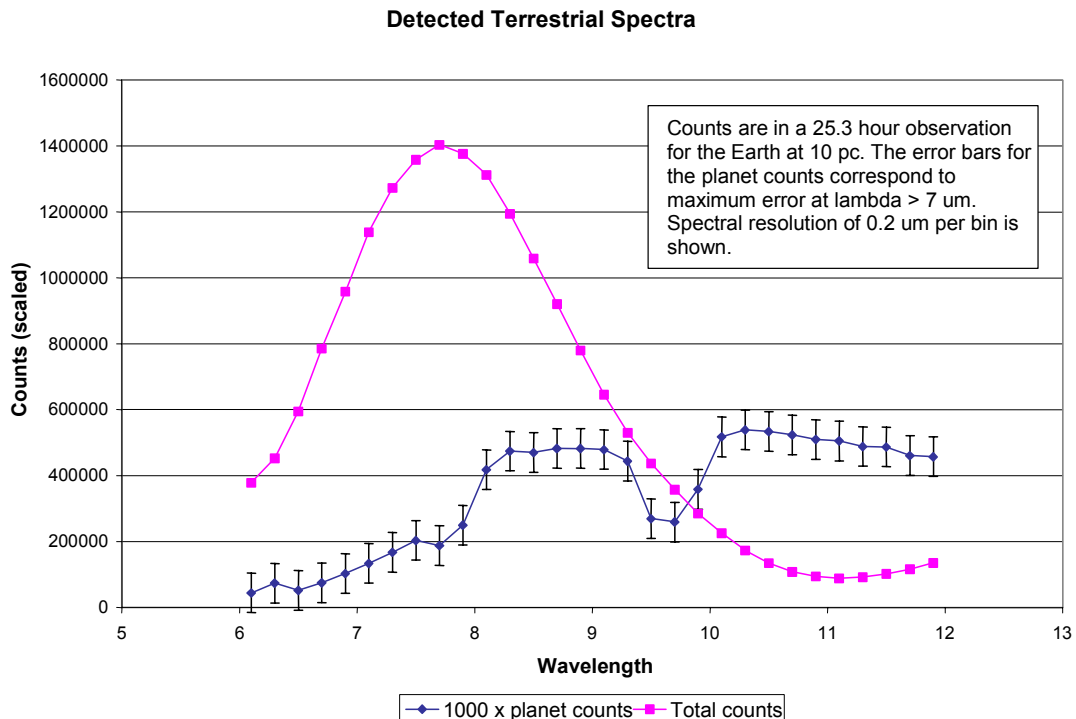
2. Spectroscopic Characterization

Using the spectrograph described above, basic observations can be taken in the 6 – 12 μm spectral band at a spectral resolution of 0.4 μm after binning in the spectral direction, corresponding to $R \approx 19$ at 7.5 μm . This will provide a minimum data set regarding the potential nature of the detected object by sampling a range of molecular lines. Specifically, lines of CO_2 , O_3 , CH_4 , H_2O and N_2O are present in that wavelength band. We have taken as a minimum performance level of achieving a $\text{SNR} = 7$ on the lines of CO_2 and O_3 at 9.31 and 9.65 μm respectively. SNR of 7 is used to allow the subtraction of the averaged continuum to give an overall $\text{SNR}=5$ in the line. We used the Earth's spectrum provided by the SWG as the input and calculated the SNR in the spectral bins used.

The table below gives the integration time required to achieve $\text{SNR}=7$ and $\text{SNR}=10$ for all wavelengths >9 μm . Follow-up observations may wish to probe for CH_4 , N_2O , H_2O (all between 7 and 8 μm) or get higher resolution observations of the CO_2 and O_3 lines. Included in the table are observation times to achieve to achieve $\text{SNR}=7$ at $\lambda > 9 \mu\text{m}$ in 0.2 μm bins and to achieve $\text{SNR}=7$ at >6.5 μm for detection of the other molecular species. The 15 pc case is excluded because of the excessively long integration times required.

Case	0.4 μm bins $\text{SNR}=7, >9$ μm	0.4 μm bins $\text{SNR}=10, >9$ μm	0.2 μm bins $\text{SNR}=7, >9$ μm	0.4 μm bins $\text{SNR}=7, >6.5$ μm
3 pc	500 seconds	900 s	1500 s	4.0 hours
5 pc	1.85 hours	4.0 hours	5.3 hours	22.4 hours
10 pc	25.3 hours	51.2 hours	81.5 hours	1143 hours
15 pc	625 hours (26 days)	1276 hours (53 days)	--	--

The plot below shows the detected spectra for the Earth at 10 pc. The error bars correspond to the maximum error in the observations for wavelengths >7 μm . The actual error is $\approx 1/2$ that shown for the wavelengths $> 10 \mu\text{m}$ due to the lower stellar flux as Poisson noise is the largest noise contributor.



3. Survey of Nearby Stars

To fully evaluate the system, a target list of 150 stars needs to be observed. The list provided by the SWG is extremely difficult for this architecture to use because of the very small inner radius of Habitable Zones that were used in the selection process. The inner working distance of this architecture is about 50 mas and less than 90 stars on the provided list have inner HZ of at least that. Our Phase I study provided a list of 162 stars with a HZ corresponding to the Earth of >75 mas, called the “Golden Oldies”. Including the entire HZ which extends $\approx 30\%$ inward of an Earth analogue orbit, the minimum HZ for that list would be 50 mas, our inner working distance. The table below lists the integration time required for a number of stars on Golden Oldies list, along with their characteristics.

Distance (pc)	Stellar Type	Angular separation	Integration time Case 1: 80 mas spot	Integration time Case 2: 60 mas spot	Integration time Case 3: 60 mas spot, separation reduced by 20 mas
12.1	G1	82 mas	53 hours	21.9 hours	175 hours
26.2	F0	88	950 s	950 s	950 s
5.9	K4	79	25.6 hours	11.1 hours	106 hours
10.1	G6	89	1900 s	950 s	2850 s
16.2	F2	139	2850 s	2850 s	2850 s
17.4	G0	76	6.1 hours	2.1 hours	35.6 hours
21.4	F5	101	2.4 hours	2.4 hours	3.96 hours
22.7	F7	80	10 hours	4.75 hours	38.8 hours

It has not been possible given the modeling tools and time available to do a detailed calculation for 150 specific target stars. This is planned to be done once the technology drivers are more fully defined and better requirements on the telescope and spacecraft performance have been specified. However, using the range of integration times required as demonstrated above, a reasonable estimate can be calculated. Should the performance against an actual target list be needed, we would wish to use the Golden Oldies list since the list provided does not cover sufficient distance. The Golden Oldies is somewhat biased towards brighter stars because the required distance to get the larger minimum HZ separations is larger. That is reflected in the selection of sources in the table. It is also obvious from the table that reaching the 50 mas separation will require either a great deal of time or an even smaller occulting spot. With a smaller spot, the dynamic range issues for the focal plane start to become severe. A more aggressive Lyot mask could help the dynamic range problem but this has not been modeled.

Based on the above values and the values obtained for the Earth / Sol system at a variety of distances, a total integration time of 24 hours per source (on average) is not too far off, assuming optimization of occulting spot and Lyot mask for each inner HZ separation. Including 2 hours to slew and acquire the target and 3 hours per target for roll maneuvers, the total integration time to survey the complete list is 181 days. This is consistent with the need to complete the detection mission in ≈ 1.5 years to allow 1 year for the characterization mission.